BBA - Molecular Basis of Disease 1871 (2025) 167601

Contents lists available at ScienceDirect

BBA - Molecular Basis of Disease

journal homepage: www.elsevier.com/locate/bbadis

A dual sensing mechanism of eastern honeybee *Apis cerana* that upregulates the expression level of chemosensory protein CSP1 and enhances the binding affinity to loquat floral volatiles at low temperature

Jia-Qi Huang [a,1], Li Zhang [a,1], Fan Wu [a], Jing Tan [a], Ping Wen [b], Wei Xu [c], Hong-Liang Li [a,*]

[a] College of Life Sciences, China Jiliang University/Zhejiang Provincial Key Laboratory of Biometrology and Inspection & Quarantine, Hangzhou 310018, China
[b] CAS Key Laboratory of Tropical Forest Ecology, Xishuangbanna Tropical Botanical Garden, Chinese Academy of Sciences, Mengla, Yunnan 666303, China
[c] School of Agricultural Sciences, College of Environmental and Life Sciences, Murdoch University, Perth, Australia

ARTICLE INFO

Keywords:
Apis cerana
Chemosensory protein
Loquat floral volatiles
Site-directed mutation
Low temperature

ABSTRACT

As a native bee species, the eastern honeybee (*Apis cerana*) plays an essential role in pollinating loquat flowers, which bloom in early winter in China. This pollination behavior is closely related to *A. cerana*'s ability to adapt to low temperatures, which depends on the functionality of its chemoreceptive system. Transcriptome analysis revealed a significant upregulation of the *A. cerana* chemosensory protein 1 (CSP1) gene at low temperatures. Fluorescence competitive binding experiments indicated that nine chemical volatiles from loquat flowers exhibited a stronger binding affinity to CSP1 than to odorant binding protein 2 (OBP2). Thermodynamic analysis revealed that CSP1's binding affinity increases at low temperatures, with a static binding mechanism largely influenced by the specific volatile molecule rather than the type of olfactory soluble protein. Molecular docking and site-directed mutagenesis confirmed that F44 residue may play a key role in CSP1's binding to three primary volatile compounds. In summary, the present study identified a dual sensing mechanism in which low temperatures upregulated the expression of CSP1 and enhanced the binding affinity of CSP1 to loquat flower volatiles. These findings not only clarify *A. cerana*'s chemoreceptive mechanism toward loquat flower volatiles in pollination but also provide a theoretical basis for further exploring ecological adaptations between native bees and early-winter flowering plants.

1. Introduction

Plants and their pollinators have undergone long processes of co-evolution and ecological adaptation in the natural environment. Honeybees are important pollinators in many natural plant ecosystems. Among them, *Apis cerana*, a native bee species of China, has experienced ecological adaptation and co-evolution as an important pollinator of Chinese native flowering plants. *A. cerana* is adept at collecting sporadic nectar sources and shows resistance to low temperatures [1], so it can still pollinate the native plants such as loquat flowers, camellias and plum blossoms that bloom in early winter in eastern China [2]. The successful reproduction of these low-temperature flowering plants relies on pollinators such as *A. cerana*, which play a crucial role in maintaining stable plant ecosystems and protecting biodiversity [3].

Loquats are native to China and are now mainly found in the hills and plains of eastern China. Loquats have a very special flowering season, generally lasting from autumn to early winter. As one of the most important nectar plants during these colder months, loquat flowers usually secrete abundant nectars rich in sucrose and release special fragrances and floral volatiles that can easily attract honeybees and other pollinators [4]. However, due to the low temperatures during the loquat flowering period, few pollinators are active in the wild, so *A. cerana* with the characteristics of low temperature tolerance is one of the main pollinators of loquat flowers. This may be due to the fact that during the long-term co-evolutionary process, *A. cerana* may have developed the ability to sense volatiles of loquat flowers even at low temperatures [5].

When pollinating insects explore plant flowers, they rely on highly efficient and complex olfactory systems [6,7]. In the olfactory chemosensillar lymph of insect chemosensory systems, a variety of soluble

* Corresponding author at: College of Life Sciences, China Jiliang University, Hangzhou 310018, China.
E-mail address: hlli@cjlu.edu.cn (H.-L. Li).
[1] These authors contributed equally to this work.

https://doi.org/10.1016/j.bbadis.2024.167601
Received 30 September 2024; Received in revised form 28 November 2024; Accepted 28 November 2024
Available online 1 December 2024

binding proteins, including odorant-binding proteins (OBPs), chemosensory proteins (CSPs), and Niemann-Pick type C2 proteins (NPC2) [8], facilitate the detection, binding and transport of small chemical molecules through the hydrophilic lymph to olfactory receptors on olfactory sensory neurons [9]. OBPs are typically highly expressed in insect antennae, whereas CSPs are expressed in various chemosensory organs such as antennae, head, thorax, abdomen and legs, where they assist in chemosensory signal transduction, embryonic development and cuticle synthesis [8].

Several OBPs and CSPs proteins are always distributed in the lymph of *A. cerana* chemosensory sensilla. In a previous study, we found that OBP2 is specifically distributed in the olfactory chemosensilla of *A. cerana* antennae [10]. OBP2 binds variety of plant volatiles [11], and its binding affinity of OBP2 for loquat floral volatiles increases at low temperature (12 °C), which supports *A. cerana*'s pollination activity in cooler weather [12]. Among the six members of the *A. cerana* CSP family members, CSP1 was significantly expressed in the antennae and head of *A. cerana* [13], and CSP1 showed a strong binding ability to plant semiochemicals like *β*-ionone [14] and the neonicotinoid imidacloprid [15]. CSP1, which was highly expressed in the antennae of *A. cerana*, may be involved in the physiological process of olfactory perception of loquat flowers. However, it remains unknown whether CSP1 is involved in the chemoreception of loquat flower volatiles by *A. cerana* at low temperatures.

In this study, antennal transcriptomic sequencing revealed that CSP1 expression is upregulated at low temperatures. Further investigation into the interaction between CSP1 and loquat floral volatiles revealed the molecular mechanism that enables *A. cerana* to detect loquat floral volatile compounds at low temperature. This study not only provides valuable insights into the molecular basis of *A. cerana*'s sensory adaptation to cold-weather flowering plants but also offers theoretical significance for understanding the co-evolutionary adaptations between insect pollinators and flowering plants in natural habitats.

2. Materials and methods

2.1. Insects, reagents and instruments

The *A. cerana* bees used in this study was reared on the campus of China Jiliang University. Approximately 300 bees were captured from the bee colony and divided into three biological replicates, with approximately 80 bees in each replicate. The replicates were placed in a 12 °C incubator for one hour. The three groups were then repeated as experimental groups. Additionally, 300 bees randomly captured at an outdoor temperature of 25 °C were divided into three groups and constituted the control group. Following a freezing period of 3–5 min at −20 °C, the tentacles were harvested and sent to Hangzhou Lianchuan Biotechnology Co., Ltd. for transcriptome sequencing.

The reverse transcription kit PrimeScript™ RT Master Mix and the fluorescence quantitative PCR kit TB Green™ Premix Ex Taq™ II (Tli RNaseH Plus) were procured from Takara Biotechnology Co., Ltd. (Takara, Shiga, Japan). *N*-phenyl-1-naphthylamine (1-NPN) was procured from TCI Company, while all volatile components of loquat floral fragrance were obtained from Shanghai Aladdin Biochemical Technology Co., Ltd. (Analytical or chromatographically pure, with a purity of ≥97 %), and methanol (HPLC grade) was procured from TEDIA Company. The site-directed mutagenesis kit Fast Mutagenesis System was procured from Beijing Quanshijin Biotechnology Co., Ltd. The pET32-CSP1 plasmid and competent BL21 (DE3) cells were prepared in-house, while all other reagents were sourced domestically.

The following instruments were used in this study. RF-5301PC fluorescence spectrophotometer (Shimadzu, Japan), a micro-volume spectrophotometer Nano Drop2000 (Thermo Scientific, USA), a real-time fluorescence quantitative PCR instrument StepOnePlus (ABI, USA), an ultrasonic disruptor and a constant temperature water bath (Ningbo Xinzhi, China).

2.2. Transcriptomics and qPCR verification of forager bees' antennae after two temperatures treatment

The total RNA was extracted from the antennae of forager bees, cDNA libraries were constructed, and RNA sequencing was performed by Hangzhou Lianchuan Biotechnology Co., Ltd. A total of six transcriptome sequencing libraries were constructed, and the effective data were assembled de novo using Trinity. The resulting unigenes were obtained after redundancy was removed. The unigenes were then aligned and annotated with sequences from the non-redundant (NR) database. The expression level of the unigenes was determined by calculating the Fragments Per Kilobase Million (FPKM) value. Genes exhibiting a difference in fold change (FC) >1.2 and a *p*-value <0.01 were identified as differentially expressed genes (DEGs). Subsequently, the OBP2 and CSP1 genes were validated through quantitative reverse transcription polymerase chain reaction (qRT-PCR) (see Table S1 for qPCR primer design), The *β*-actin gene was used as a reference gene. The cDNA was diluted to 100 ng/μL with ddH_2O, and the reaction system (20 μL) was performed according to the fluorescent quantitative PCR kit. The reaction procedure was as follows: predenaturation at 95 °C for 30 s, followed by 40 cycles of denaturation at 95 °C for 5 s, annealing and extension at 60 °C for 30 s. The relative expression of the genes was determined using the $2^{-\Delta\Delta Ct}$ method.

2.3. Expression and purification of CSP1 recombinant protein

The recombinant plasmid pET32-CSP1 was re-transfected into *E. coli* BL21 (DE3) competent cells in accordance with the previously described method [14]. The single positive colonies were verified and inoculated into LB medium at 37 °C. Once the OD_{600} value reached 0.6, isopropyl-β-d-thiogalactoside (IPTG) was added at a final concentration of 1 mM, and the mixture was incubated at 30 °C for a period of 5 h. The bacterial culture was then collected for ultrasonic disruption, and the target protein was detected by sodium dodecyl sulphate-polyacrylamide gel electrophoresis (SDS-PAGE). The recombinant CSP1 protein was separated and purified using a nickel agarose column containing different concentrations of imidazole. Following dialysis with PBS, the recombinant CSP1 protein was stored at −20 °C in preparation for subsequent experiments.

2.4. Fluorescence competition binding assay

In this study, 1-NPN was used as a fluorescent reporter, referred to the previous method [12]. The aim was to determine the dissociation constants of the CSP1 recombinant protein and nine common floral chemical volatile molecules in loquat flowers. The floral fragrance volatile molecules, at a concentration of 1 mM, were added to a mixed solution of 1-NPN and CSP1 recombinant proteins in sequence. The maximum fluorescence emission intensity of the mixed system was recorded simultaneously, and the dissociation constant K_D of each volatile molecule and CSP1 was calculated according to the formula [16] below,

$$K_D = \frac{[IC_{50}]}{1 + \frac{[1-NPN]}{K_{1-NPN}}} \quad (1)$$

where $[IC_{50}]$ is the concentration of the ligand when the fluorescence intensity of 1-NPN drops to half, [1-NPN] is the concentration of free 1-NPN in the system, and $K_{1\text{-NPN}}$ is the dissociation constant of the CSP1 recombinant protein with 1-NPN.

2.5. Thermodynamic assays of CSP1 recombinant protein and three loquat floral volatiles

Based on the results of the fluorescence competitive binding experiment, and referring to a previous method [14], thermodynamic assays

were used to study the binding interactions of CSP1 with the three strongest loquat floral volatiles (4-methoxybenzaldehyde, (*E*)-ethyl cinnamate, and methyl cinnamate) at two temperatures of 285 K and 298 K, respectively. The CSP1 recombinant protein was added to a 3 mL quartz cuvette and titrated with three loquat floral volatile molecules. The fluorescence emission spectra were scanned and the fluorescence intensity at the maximum emission wavelength was recorded. According to the Stern-Volmer equation [17] (formula 2) and the double LOG equation [18](formula 3), the quenching constant K_{SV} value and the apparent binding constant K_A value were calculated to determine the fluorescence quenching mechanism.

$$\frac{F_0}{F} = 1 + K_q \tau_0 [Q] = 1 + K_{SV} \tag{2}$$

$$lg\frac{F_0 - F}{F} = lgK_A + nlg \tag{3}$$

In the two equations, F_0 and F are the fluorescence intensities of the system before and after the quencher is added, respectively; [Q] is the quencher concentration; K_q is the fluorescence quenching rate constant; τ_0 is the average lifespan of the fluorescence molecule when no quencher is added; *and* K_{SV} is the dynamic quenching constant of the Stern-Volmer equation. The K_{SV} value increases with an increase in temperature, which is dynamic quenching, while the K_{SV} value decreases with an increase in temperature, which is static quenching [19]; n is the binding number of sites; *and* K_A is the apparent binding constant.

In addition, the interaction between proteins and small-molecule compounds can be calculated using the Gibbs free energy (ΔG), enthalpy change (ΔH), and entropy change calculated by thermodynamic formulas (4), (5), and (6). (ΔS) is reflected by three thermodynamic parameters, mainly including hydrogen bonds, van der Waals forces, electrostatic forces and hydrophobic interactions [20],

$$\Delta G = -RTlnK = \Delta H - T\Delta S \tag{4}$$

$$\Delta H = \frac{RT_1T_2ln(K_{0.2}/K_{0.1})}{T_2 - T_1} \tag{5}$$

$$\Delta S = (\Delta H - \Delta G)/T \tag{6}$$

where R is the gas constant, T is the thermodynamic temperature (T_1 and T_2 are the two temperatures in the experiment), K is the binding constant, and $K_{0,\ 1}$ and $K_{0,\ 2}$ are the binding constants at T_1 and T_2, respectively. The determination of the main force type between the protein and ligand is reflected by the positive and negative values of ΔH and ΔS [14]. When $\Delta H < 0$ and $\Delta S > 0$, the binding force type is hydrophobic interaction and electrostatic force; when $\Delta H < 0$ and $\Delta S < 0$, the force is a hydrogen bond and van der Waals force; $\Delta H > 0$ and $\Delta S > 0$, which is a typical hydrophobic interaction.

2.6. Molecular docking

The crystal structure data of the CSP1 protein were predicted and obtained using the SWISS-MODEL [21] online website. The 3D structures of 4-methoxybenzaldehyde (CID number: 31244), methyl cinnamate (CID number: 637520), and (*E*)-ethyl cinnamate (CID number: 637758) from the PubChem database using Molegro Virtual Docker 4.2 software (free trial) performs molecular docking, compare the energy values contributed by different amino acids based on the docking results, and identify possible key amino acids.

2.7. Site-directed mutagenesis

Site-directed mutation primers (Table S2) were designed, and a site-directed mutation kit was used to perform the mutations based on the recombinant plasmid pET32-CSP1. The PCR program was as follows: 95 °C for 3 min, 95 °C for 20 s, 55 °C for 20 s, 72 °C for 3 min, 25 cycles, and 72 °C for 10 min. The PCR products were detected using 1 % agarose gel electrophoresis and digested with DMT. The two CSP1 mutagenesis plasmids were sequenced and verified, and the two CSP1 recombinant mutant proteins were induced and purified according to the method described in Section 2.3.

2.8. Interaction and thermodynamic analysis of two CSP1 mutant proteins and loquat floral volatile molecules

The thermodynamic analysis methods outlined in Section 2.4 were employed once more to examine the interaction between two CSP1 mutant proteins and three loquat flower volatiles, namely 4-methoxybenzaldehyde, (*E*)-ethyl cinnamate, and methyl cinnamate. The thermodynamic parameters were then calculated and compared with those of the wild-type CSP1 protein.

2.9. Data processing

All original data were organized using Microsoft Excel 2010, and GraphPad Prism software (version 8.0) was used to plot all figures and calculate the significance of all the data ($p < 0.05$).

3. Results

3.1. Expression analysis of differential genes in transcriptome

Six transcriptome raw data were obtained from the corresponding six *A. cerana* antennal sequencing libraries. After filtering the raw data of the samples, namely removing sequencing adapters and low-quality sequences, the effective valid read was >3.4 × 10 [7]. The proportion of valid readings was >94.88 %, the proportion of Q20 base was 99.98 %, the proportion of Q30 base was >97.58 %, and the GC content was between 38 % and 39 % (Table 1). This indicates that the data quality of each library is suitable for subsequent analysis.

In the transcriptome analysis, the 12, 319 Unigenes were normalized by calculating FPKM values, setting at FC > 1.2, and *p-value* < 0.01, to screen for differentially expressed genes (DEGs). A total of 4694 DEGs were identified. The overall distribution of these DEGs was illustrated in the volcano plot (Fig. 1-A). This includes genes that were significantly differentially expressed (red), genes that were only differentially up-regulated without significant *p-values* (light red), and genes that significantly differentially expressed with down-regulated expression (blue), as well as genes that were only differentially down-regulated genes without significant *p-values* (light blue). The number of genes in each category were as follows: 65, 2630, 172, and 1827, respectively. It was observed that *OBP2* expression was significantly decreased following treatment 12 °C (blue point labelled), whereas *CSP1* expression was upregulated after treatment at 12 °C (light red point labelled). Quantitative polymerase chain reaction (qPCR) was employed to validate the expression trends of the two genes, which were in accordance with the transcriptome sequencing results. Furthermore, *CSP1* demonstrated a markedly up-regulation expression following treatment at 12 °C, while *OBP2*, was significantly downregulated under the same temperature (Fig. 1-B, analysis of variance, $p < 0.05$).

Table 1
Statistical table of RNA-Seq data quality.

Sample	Valid Reads	Valid Base	Valid Ratio %	Q20%	Q30%	GC%
AcAn25d_1	45,908,152	6.89G	95.44	99.98	97.60	39
AcAn25d_2	39,453,288	5.92G	94.88	99.98	97.65	38.50
AcAn25d_3	34,029,708	5.10G	95.30	99.98	97.58	38.50
AcAn12d1_1	37,509,178	5.63G	94.99	99.98	97.65	38
AcAn12d1_2	46,704,806	7.01G	95.29	99.98	97.66	38.50
AcAn12d1_3	48,752,316	7.31G	95.28	99.98	97.65	38

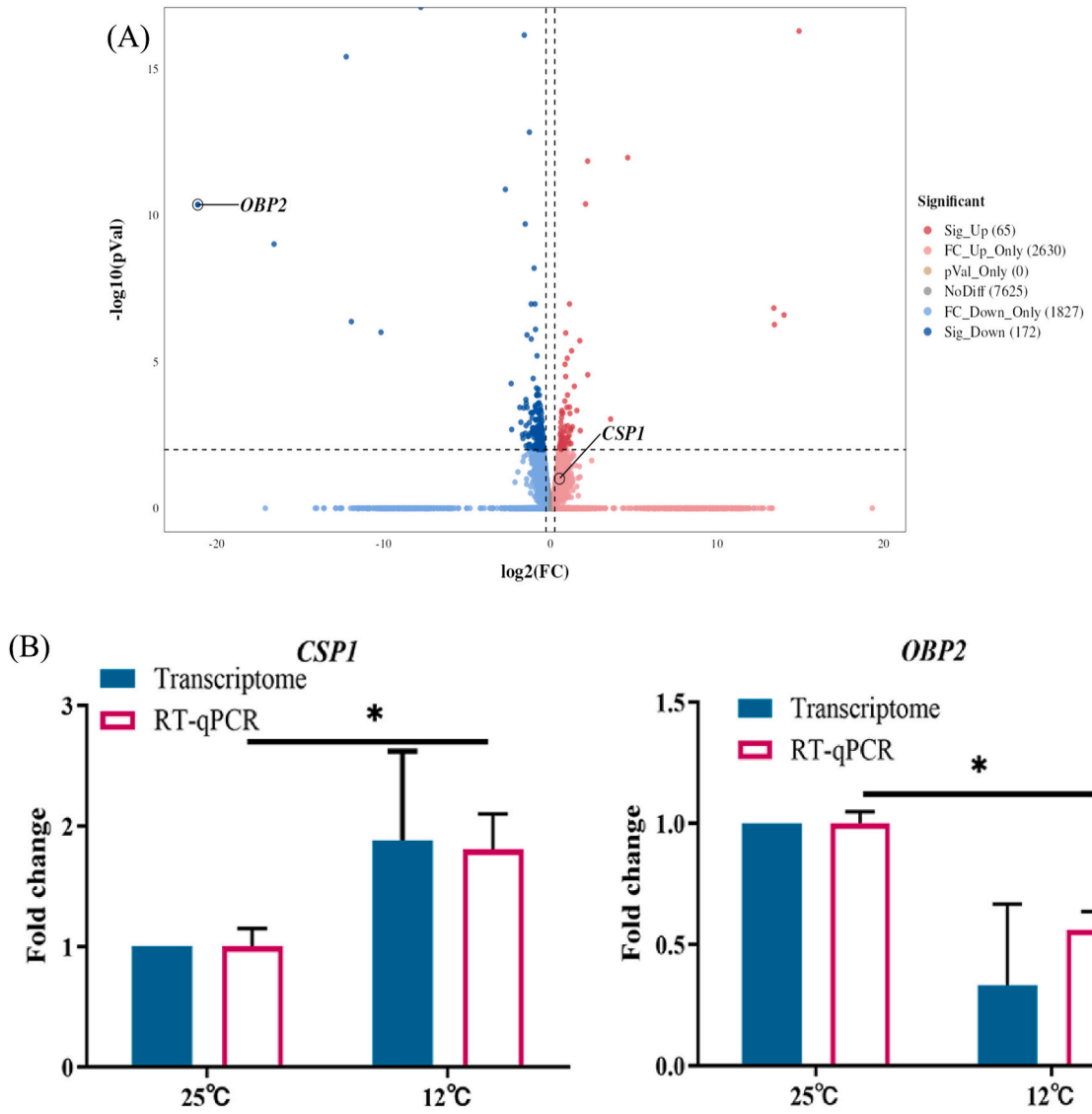

Fig. 1. Gene Expression Analysis: Volcano Plot (A) and qPCR (B).
Note: (A) The abscissa represents the fold change of gene expression in different samples, and the ordinate represents the statistical significance of the change of gene expression. (B) qRCR validation of *CSP1* and *OBP2* genes in the antennary cold-sensing transcriptome ($p < 0.05$).

3.2. Purification of CSP1 recombinant protein

The recombinant CSP1 protein was successfully expressed, purified, and confirmed by SDS-PAGE analysis. As illustrated in Fig. 2-A, lanes 1 and 2 showed the extracted proteins from *E. coli* in the absence of IPTG and following IPTG induction, respectively. Lanes 3 and 4 demonstrated the supernatant and pellet, respectively, following the ultrasonic disruption of the bacterial culture. The purified CSP1 recombinant protein exhibited a molecular weight of approximately 29.0 kDa (Fig. 2-B). The final concentration of the recombinant CSP1 protein was adjusted to 1 μmol•L^{-1} for subsequent experiments.

3.3. Fluorescence competitive binding experiment

The maximum excitation wavelength of the CSP1 recombinant protein was determined to be 282 nm. In the competitive fluorescence binding experiment, the fluorescence intensity of the CSP1–1-NPN mixed solution was recorded at a wavelength of approximately 430 nm. The dissociation constant ($K_{1\text{-NPN}}$) and the number of binding sites (n) were calculated to be 2.89 μmol·L^{-1} and 0.847, respectively. A high degree of linear correlation was observed (Fig. 3-A, B). Furthermore,

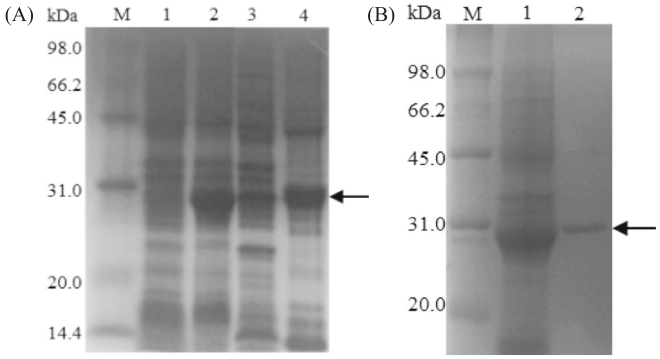

Fig. 2. Expression and Purification of *CSP1* Protein.
Note: Lane M is protein molecular weight Marker. (A). lane 1 and 2 are the uninduced and induced bacterial lysis products, respectively. Lane 3 and 4 were bacterial lysis supernatant and inclusion body lysate, respectively. Lane 2 of Fig. B shows the purified CSP1 recombinant protein. The black arrow points to the relevant band of *CSP1* recombinant protein.

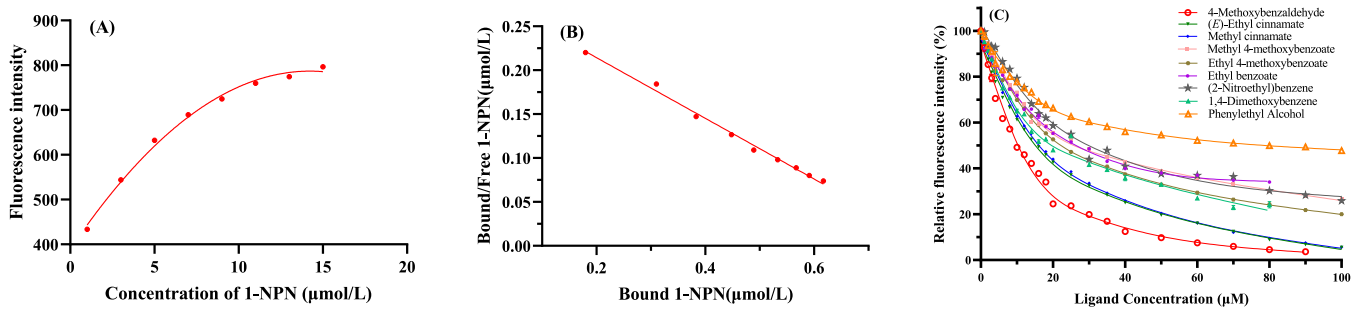

Fig. 3. Fluorescence spectra (A) and Scatchard curve (B) of the CSP1 recombinant protein binding with different concentrations of fluorescence reporter 1-NPN, loquat flower volatiles (C) competed with the complex of CSP1–1-NPN.

nine candidate chemical volatiles present in loquat flowers were observed to competitively quench the fluorescence of CSP1–1-NPN. The relative fluorescence intensity of 1-NPN was found to be reduced to <50 % in the presence of all floral volatiles (Fig. 3-C). The IC_{50} and K_D values for each volatile are presented in Table 2.

Of the nine identified loquat floral volatiles, three exhibited particularly strong competitive binding abilities, with 4-methoxybenzaldehyde, (*E*)-ethyl cinnamate and Methyl cinnamate demonstrating the greatest affinity, competing with the relative fluorescence intensity of 1-NPN to a degree of <20 %. The dissociation constant (K_D) values with CSP1 reach 2.07 μmol/L, 3.03 μmol/L and 3.22 μmol/L, respectively (Table 2; the corresponding parameters of OBP2 from the previous study were also listed for comparison). In light of the data presented in Table 2, it can be found that these three loquat floral volatiles may play a pivotal role in the olfactory sensing mechanism of loquat flowers perceived by *A. cerana*.

3.4. Thermodynamic analysis of CSP1 protein binding to loquat floral volatiles

To further elucidate the binding interaction between CSP1 and loquat floral volatiles, a thermodynamic analysis was conducted to the recombinant protein CSP1 with the three most significant loquat floral volatiles, 4-methoxybenzaldehyde, (*E*)-ethyl cinnamate, and methyl cinnamate. This thermodynamic analysis used fluorescence spectrometry at 285 K and 298 K, respectively. The results are presented in Fig. 4. At the maximum emission wavelength of 340 nm, the fluorescence intensity of CSP1 was observed to decrease in a regular manner with the increasing concentration of the compounds, which indicated that there was a strong binding interaction between CSP1 and the three loquat floral volatiles. Subsequent calculations using the Stern-Volmer equation revealed that the K_{SV} values of CSP1 and the three loquat floral volatiles exhibited a decline with rising temperature (Fig. 5). This suggests that the interaction between the two is a static quenching process. The binding constant, K_A, and the number of binding sites, *n*, between CSP1 and the three volatile molecules were calculated using formulas (2) and (3). As illustrated in Table 3, the number of binding sites (*n*) between CSP1-WT and the three volatile molecules was approximately one. 4-methoxybenzaldehyde demonstrated the strongest binding affinity for CSP1, followed by methyl cinnamate and (*E*)-ethyl cinnamate. These findings suggested that the binding of volatile molecules with diverse structures to the CSP1 protein was subject to certain specificity and selectivity, which may be related to the detailed binding sites of these volatile molecules to the amino acid sites of the CSP1 protein.

Table 2
Binding assay of candidate semiochemicals with the recombinant CSP1 and OBP2 [12] protein.

Loquat floral volatiles	[IC_{50}](μmol/L)		K_D (μmol/L)	
	CSP1	OBP2	CSP1	OBP2
4-methoxybenzaldehyde	10.32	20.74	2.07	7.46
(*E*)-ethyl cinnamate	15.11	26.77	3.03	9.63
methyl cinnamate	16.06	32.06	3.22	11.54
1, 4-dimethoxybenzene	20.83	–	4.18	–
ethyl 4-methoxybenzoate	22.17	–	4.45	–
methyl 4-methoxybenzoate	25.72	74.23	5.16	26.71
ethyl benzoate	26.31	–	5.28	–
(2-nitroethyl)benzene	28.02	89.04	5.62	32.04
phenylethyl alcohol	78.57	–	15.77	–

3.5. Molecular docking

The three-dimensional structure of CSP1 was predicted using the crystal structure of *Spodoptera exigua* CSP MbraA6 (1n8v.2.A) on the SWISS-MODEL website as a template. The degree of similarity between the CSP1 sequence and the template was 38.04 %, and the GMQE value was 0.65, indicating that the modeling was of considerable reliability. The results of the molecular docking of CSP1 and three loquat floral volatiles are illustrated in Fig. 6. The results indicated that the two amino acids, Phe44 (F44) and Gln63 (Q63), were the most energetically significant during the binding process between CSP1 and the three floral volatiles (Fig. 6-A). Based on these findings, F44 and Q63 were identified as mutation sites of CSP1, and a three-dimensional model of CSP1 binding to three volatile molecules was constructed (Fig. 6-B, C, D).

3.6. Site-directed mutagenesis

Based on the predicted two key amino acid sites, site-directed mutation primers were designed to mutate the wild-type CSP1 plasmid, with the objective of mutating the target amino acid into glycine. The recombinant proteins CSP1-F44 and CSP1-Q63, which had undergone a single amino acid mutation, were obtained through prokaryotic expression induction and purification. The two mutant proteins were finally identified by SDS-PAGE (Fig. 7). Lanes 1 and 2 represent the mutant CSP1-F44 and CSP1-Q63, respectively, with an estimated molecular weight of approximately 29.0 kDa. The final concentration of the two mutant CSP1 proteins was adjusted to 1 μmol•L^{-1} for subsequent experiments.

3.7. Thermodynamic analysis of CSP1 mutant protein binding to loquat floral volatiles

To confirm the precision of key amino acid residues, two CSP1 mutant proteins and three loquat flower volatile compounds underwent a further thermodynamic analysis. The binding constant (K_A), the number of binding sites (*n*), and the percentage decrease of the wild-type and mutant protein CSP1 were calculated in accordance with formulas 2 and 3. As illustrated in Fig. 8 and Table 3, the number of binding sites (*n*) of the two CSP1 mutant proteins interacting with all three volatile compounds was found to be approximately equal to one. Furthermore, the K_A values of mutant CSP1-F44G binding to all three floral volatile compounds were reduced by 59.26 %, 53.39 %, and 38 %, respectively,

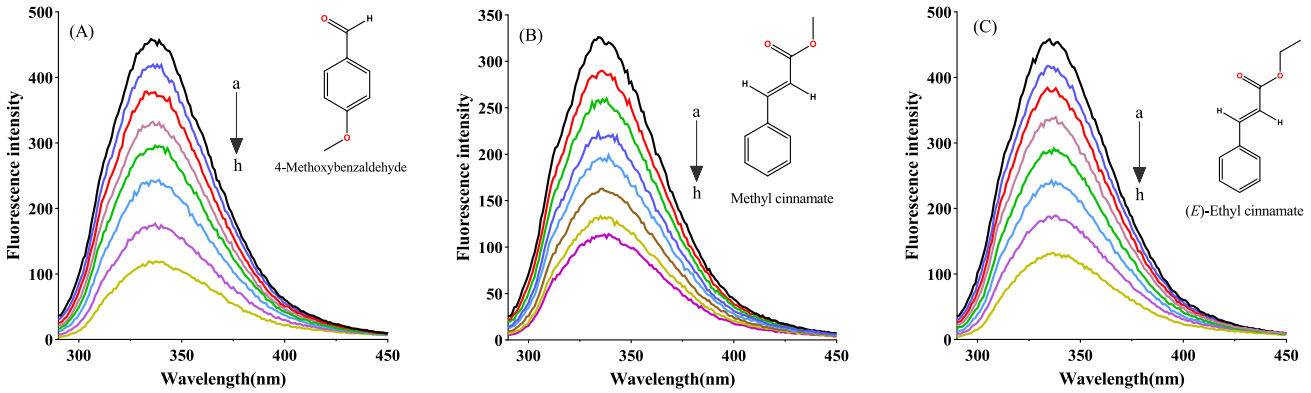

Fig. 4. Fluorescence quenching spectra of CSP1 binding with 4-methoxybenzaldehyde (A), Methyl cinnamate (B) and (*E*)-ethyl cinnamate (C).Note: a-h means that the fluorescence peak of CSP1 recombinant protein gradually decreases as the concentration of ligand increases.
Note: a-h represents a gradual decrease in fluorescence intensity of *CSP1* recombinant protein with increasing ligand concentration.

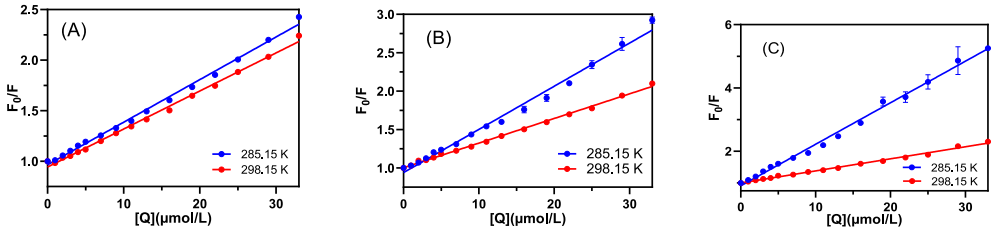

Fig. 5. Stern-Volmer diagram of 4-methoxybenzaldehyde (A), methyl cinnamate (B) and (*E*)-ethyl cinnamate (C) binding with CSP1 recombinant protein. Note: All slopes regularly change according to the calculation of the Stern-Volmer Equation at two different temperatures.
Note: All slopes change regularly at two different temperatures as calculated by the Stern-Volmer equation.

Table 3
The apparent association constant (K_A) and the number of binding sites (n) of CSP1, CSP1-F44G, and CSP1-Q63G.

Loquat floral volatiles	Proteins	Double LOG equations			
		K_A ($\times 10^4$ L·mol^{-1})	n	R^2	Decline rate(%)
4-methoxybenzaldehyde	CSP1-WT	2.855	1.077	0.9966	–
	CSP1-F44G	1.163	1.339	0.9976	59.26
	CSP1-Q63G	1.74	1.200	0.9977	39.05
methyl cinnamate	CSP1-WT	4.716	0.877	0.9956	–
	CSP1-F44G	2.198	1.076	0.9978	53.39
	CSP1-Q63G	3.139	0.968	0.9972	33.44
(*E*)-ethyl cinnamate	CSP1-WT	4.092	0.971	0.9934	–
	CSP1-F44G	2.537	1.097	0.9915	38
	CSP1-Q63G	3.914	0.961	0.9931	4.34

in comparison to the wild-type CSP1. Similarly, the K_A values of mutant CSP1-Q63G were reduced by 39.05 %, 33.44 %, and 4.34 %, respectively. This suggests that the binding forces of the two mutant proteins to the three volatiles were all weakened. In particular, the role of Phe44 in the interaction between CSP1 and the three loquat floral volatiles was found to be of particular significance.

The role of key amino acids in the interaction between CSP1 proteins and loquat floral volatile molecules was subjected to further analysis. As illustrated in Table 4, the K_{SV} of the wild-type and mutant proteins exhibited a decline with increasing temperature, suggesting that the interaction between the wild-type and mutant CSP1 proteins and the volatiles was of the static quenching type. In comparison to the wild-type CSP1 protein, the interactions between CSP1-F44G and CSP1-Q63G proteins and 4-methoxybenzaldehyde underwent a transition from hydrophobic interactions and electrostatic forces to hydrogen bonds and van der Waals forces. This suggests that F44 and Q63 may play a role in the hydrophobic interaction and electrostatic interaction of CSP1 binding with 4-methoxybenzaldehyde. The interaction between CSP1-F44G and CSP1-Q63G proteins and methyl cinnamate underwent a shift from hydrophobic interaction to hydrogen bonding and van der Waals forces. This suggests that F44 and Q63 may serve as crucial amino acids in maintaining the hydrophobic interaction between CSP1 and methyl cinnamate. The interaction between CSP1-F44G and CSP1-Q63G with (*E*)-ethyl cinnamate remains unaltered by hydrogen bonds and van der Waals forces.

4. Discussion

As a nectar plant that blooms in winter, the loquat flower relies on insect pollination from Apidae and Syrphidae families. The Apidae family, which accounts for 67.89 % of the pollinators, is responsible for the majority of pollination activity, while Syrphidae, which accounts for 21.57 % of the total, also plays a significant role [4]. These insects are of critical importance for maintaining loquat orchard yields and fruit quality. A notable decline in the abundance of primary pollinators in loquat orchards can result in a reduction in loquat yield and quality, as

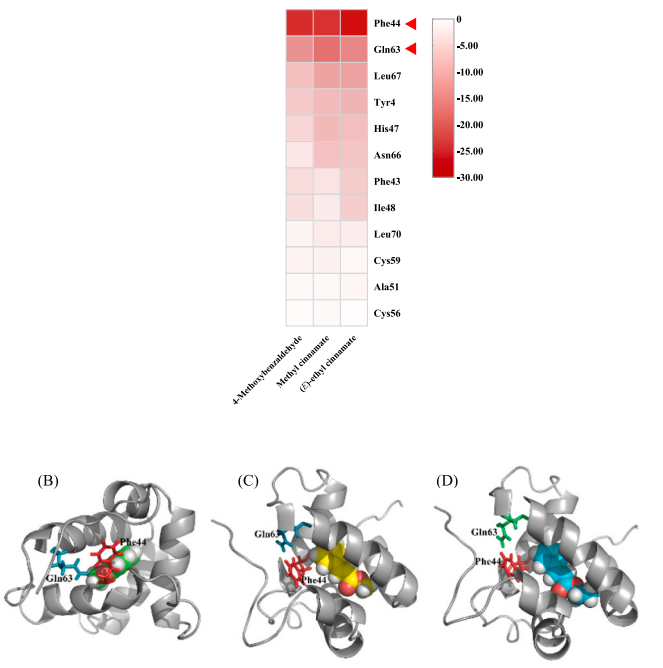

Fig. 6. Amino acid energy contribution of CSP proteins (A) and molecular docking (C-E).
Notes: (A). Energy contributions of amino acid residues of *CSP1* protein when docking with 4-methoxybenzaldehyde, Methyl cinnamate and (*E*)-ethyl cinnamate, respectively. Molecular docking results of *CSP1* protein with 4-methoxybenzaldehyde (B), methyl cinnamate (C) and (*E*)-ethyl cinnamate (D), respectively.

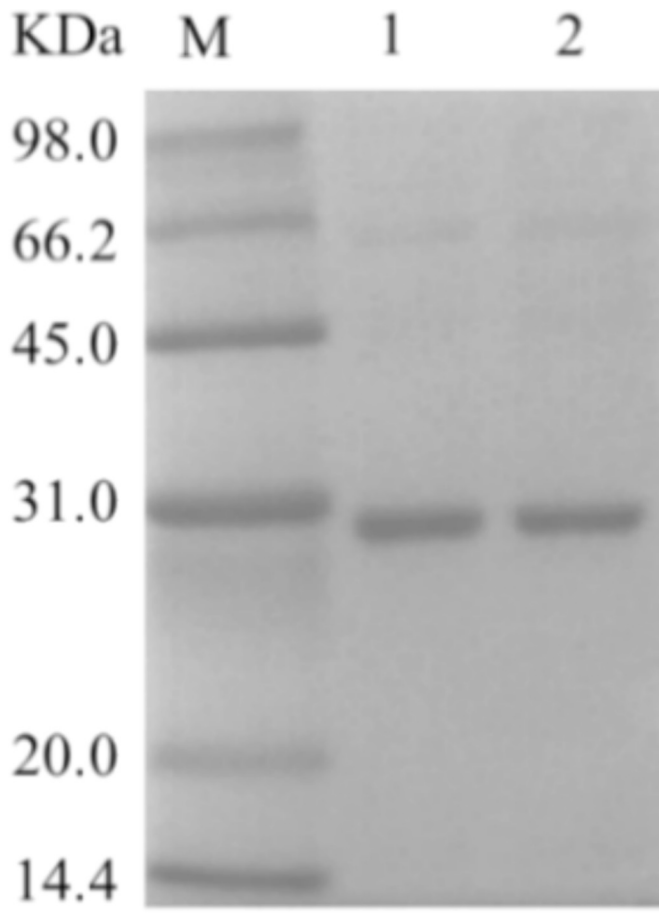

Fig. 7. Purification of the mutant protein *CSP1*.
Note: Lane M is protein molecular weight Marker. Lane 1 is the purified *CSP1*-F44G and lane 2 is the *CSP1*-Q63G mutant histone.

well as substantial losses in agricultural production [2]. Therefore, studying the insect pollination mechanisms is crucial to ensure a bumper harvest and increase production of loquats. The blooming period of loquat is nearly early winter in East China, occurring at relatively low temperatures (approximately 12 °C). Over the course of its evolutionary history, *A. cerana* has demonstrated robust cold tolerance and the capacity to survive in low-temperature conditions. This resilience may be attributed to the distinctive physiological mechanisms that enable *A. cerana* to tolerate low temperatures [22,23].

The pollination behavior of *A. cerana* is primarily guided by its olfactory system. In a previous study, we demonstrated that OBP2 can enhance the binding affinities with loquat floral volatiles at low temperatures [12]. To further investigate the olfactory sensing mechanism of *A. cerana* at low temperatures, this study compared the transcriptome of the antennae of *A. cerana* foragers treated at low temperature (12 °C) and high temperature (25 °C), respectively. Notably, the expression of OBP2 was observed to be markedly diminished in response to the low-temperature treatment (Fig. 1-A, C). These findings suggest that while the affinity of OBP2 for floral volatiles may increase at low temperatures, the significant decrease in expression level may limit *A. cerana*'s ability to detect loquat volatiles at low temperatures. Interestingly, transcriptome data revealed a significant up-regulation of CSP1, a gene previously identified as highly abundant in the antennae of *A. cerana* [13], in response to low temperatures (Fig. 1-A, B). This suggests that CSP1 may play a key role in enhancing *A. cerana* sensing capabilities at low temperatures. To further investigate the recognition mechanism of *A. cerana* to flowering plants at low temperatures, this study analyzed the binding interaction between CSP1 and main loquat floral volatiles through biochemical binding, thermodynamic assays, and site-directed mutagenesis. These findings provide a theoretical basis for the co-evolutionary relationship between honeybee pollinators and flowering plants under unfavorable conditions.

The binding affinities between the CSP1 protein and loquat floral volatiles demonstrated that all nine loquat flower volatile molecules exhibited competitive binding with the relative fluorescence value of the fluorescent reporter 1-NPN, with an intensity of <50 %. In comparison to the results obtained for OBP2 [12], the K_D values for CSP1 binding with all loquat floral volatiles were found to be less than that of OBP2 (Table 2). This suggested that CSP1 may play a more prominent role than OBP2 in the olfactory sensing of loquat floral volatiles by *A. cerana*. Among the nine volatiles, 4-methoxybenzaldehyde, methyl cinnamate and (*E*)-ethyl cinnamate exhibited the strongest binding abilities with the CSP1 protein, as evidenced by the static binding mechanism, which was in accordance with the OBP2 results [12]. This finding indicated that these three compounds were indeed the key floral volatiles of loquat flowers that attract *A. cerana* to visit. A comparable phenomenon was observed in the chemoreception of *Halyomorpha halys*, wherein HhalCSP15 [24] and five HhalOBPs [25] exhibited a comparable strong binding affinity with the same plant volatile β-ionone. This indicates that despite the structural dissimilarities between olfactory-related proteins (CSPs or OBPs) in different insects, their functions exhibit certain commonalities in recognizing key volatiles. In this study, we found that CSP1 protein of *A. cerana* plays a more significant role than OBP2 in the recognition of loquat floral volatiles. These findings highlight the importance of olfactory related proteins in insect host selection and environmental adaptation, as well as their recognition mechanisms, which are conserved across different insects.

In order to further reveal the key amino acid sites and interaction mechanisms between CSP1 and the three loquat floral volatile molecules, this study used molecular docking to predict the two potential key amino acids, Phe44 and Gln63. Following the generation of the CSP1-

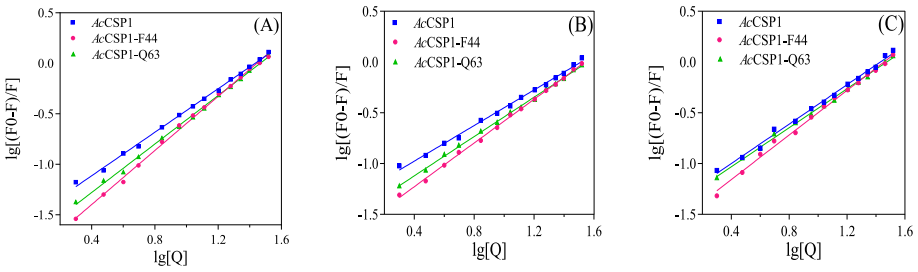

Fig. 8. Double LOG Plot of Fluorescence Quenching for *CSP1* and Its Mutant Proteins with 4-methoxybenzaldehyde (A), methyl cinnamate (B) and (*E*)-ethyl cinnamate (C).

Table 4
Quenching mechanisms and thermodynamic parameters of CSP1 and its two mutants with three loquat floral volatiles.

Loquat floral volatiles	Protein	T/K	K_{SV} ($\times 10^4$ L·mol^{-1})	K_A ($\times 10^4$ L·mol^{-1})	Thermodynamic parameter			Binding force
					ΔH (kJ·mol^{-1})	ΔS (J·mol^{-1}·K^{-1})	ΔG (kJ·mol^{-1})	
4-methoxybenzaldehyde	CSP1-WT	285	4.21	3.37	−22.81	6.63	−24.70	HE
		298	3.84	2.85			−24.74	
	CSP1-F44G	285	4.48	3.42	−148.14	−432.99	−24.74	HV
		298	3.63	1.16			−22.57	
	CSP1-Q63G	285	4.19	2.47	−48.45	−85.88	−23.97	HV
		298	3.65	1.73			−23.54	
methyl cinnamate	CSP1-WT	285	5.30	4.16	16.79	147.38	−25.21	HI
		298	3.17	4.72			−25.95	
	CSP1-F44G	285	6.33	4.80	−107.39	−287.17	−25.54	HV
		298	2.93	2.19			−24.11	
	CSP1-Q63G	285	6.12	6.56	−101.32	−263.28	−26.28	HV
		298	2.84	3.14			−24.97	
(*E*)-ethyl cinnamate	CSP1-WT	285	12.47	10.40	−128.22	−353.84	−27.37	HV
		298	3.83	4.09			−25.61	
	CSP1-F44G	285	7.63	7.26	−144.49	−413.92	−26.52	HV
		298	2.96	2.54			−24.45	
	CSP1-Q63G	285	6.79	7.01	−80.09	−188.26	−26.44	HV
		298	3.43	3.91			−25.50	

HV: Hydrogen bonds and Van der Waals force.
HE: Hydrophobic and electrostatic force.
HI: Hydrophobic interaction.

F44G and CSP1-Q63G mutant proteins, we used fluorescence quenching and thermodynamic analysis to substantiate the potential role of the two key amino acid sites. As shown in Table 3, compared with CSP1 wild-type, the K_A values of the CSP1-F44G mutant in complex with 4-methoxybenzene and methyl cinnamate were found to decrease by 59.26 % and 53.39 %, respectively, which was much higher than the K_A value of CSP1-Q63G (39.05 % and 38 %, respectively). This suggests that F44 plays a more pivotal role in CSP1 and the three loquat floral volatiles. This finding is in accordance with the amino acid binding energy prediction of molecular docking (Fig. 6-A), as well as the previously reported key amino acid positions of CSP1 binding with β-ionone [14].

It has been demonstrated that key amino acids in insects' CSPs invariably perform indispensable functions in the perception of plant volatiles. For example, Val48 and Thr66 in BodoCSP1 in *Bradysia odoriphaga* were identified as the key binding site for host plant volatiles through site-directed mutagenesis [26]. AgifCSP5 may be involved in the detection of aphid-infested crops from long distances by *Aphidius gifuensis*, which binds to trans-2-nonenal, with Tyr75 identified as the key amino acid [27]. Through site-directed mutagenesis and ligand binding experiments, it was confirmed that Thr27 in GmolCSP8 of *Grapholita molesta* was the key binding site for 1-hexanol. This was because this residue was able to form a hydrogen bond with the oxygen atom of the hydroxyl group in 1-hexanol [28]. These findings highlighted the importance of key amino acid residues in insect CSPs for their ability to bind plant volatile compounds.

With regard to the binding mechanism, the wild-type and mutant CSP1 proteins were observed to undergo a static quenching process when combined with the three loquat floral volatiles. This is in accordance with OBP2 binding to the same volatiles [12], while contrasts with the dynamic binding of and CSP1 as well as OBP2 observed for β-ionone [14,29]. This suggests that the binding mechanism mainly depends on the type of specific volatile molecule rather than the type of olfactory soluble protein. In terms of interaction forces, the two mutant proteins, CSP1-F44 and CSP1-Q63, exhibited hydrogen bonding and van der Waals forces with the three loquat flower volatiles, regardless of the forces observed in the wild type (Table 4). Furthermore, for the interaction with β-ionone, the binding force changing result was similar to CSP1-Q63, while differ from CSP1-F44 [14], thus demonstrating the diversity of driving forces that govern the binding of the CSP1 protein to different plant volatile molecules. This diversity may be related to the diversity of chemical structures of odor molecules [11].

Our previous study demonstrated that OBP2 exhibited enhancing affinity for loquat volatiles at low temperatures, thereby facilitating the olfactory perception of loquat floral substances by *A. cerana* at low temperatures [12]. However, the FPKM value of OBP2, as indicated by the transcriptome sequencing results, exhibits a notable decline at low temperatures. Conversely, the FPKM value of CSP1 demonstrates an increase at low temperatures (Fig. 1). To comprehensively evaluate the impact of gene expression and binding affinity on the binding of proteins to loquat flower volatiles, we multiplied the K_A and FPKM of each loquat floral volatile for the two proteins, respectively. As shown in Table 5, the multiplication of CSP1 and OBP2 demonstrated an up-regulation and down-regulation, respectively, compared to high temperate (298 K/ 25 °C). This further illustrates that gene expression at low temperatures

Table 5
Comparison of comprehensive sensing abilities of CSP1 and OBP2 [12] with 4-Methoxybenzaldehyde, Methyl cinnamate, and (*E*)-Ethyl cinnamate at 285 K and 298 K.

Loquat floral volatiles	Proteins	*T*/K	K_A($\times 10^4$ L·mol^{-1})	FPKM	K_A × FPKM	Comprehensive sensing abilities
4-methoxybenzaldehyde	CSP1	285	3.37	2750.16	9268.1	↑
		298	2.85	1882.19	5346.2	
	OBP2	285	4.17	0.02	0.0834	↓
		298	2.79	232.15	647.69	
methyl cinnamate	CSP1	285	4.16	2750.16	11,440.6	↑
		298	4.72	1882.19	8883.9	
	OBP2	285	4.97	0.02	0.0994	↓
		298	4.90	232.15	1137.5	
(*E*)-ethyl cinnamate	CSP1	285	10.40	2750.16	28,601.7	↑
		298	4.09	1882.19	7698.2	
	OBP2	285	6.33	0.02	0.1266	↓
		298	3.71	232.15	861.3	

Note: The comprehensive abilities of sensing odor mean the products of the binding affinity of the olfactory related protein with the volatiles and the FPKM value of the gene expression. Whichever increase or decline is the result of low temperatures versus high temperatures. CSP1 showed the more comprehensive abilities to sense loquat flower volatiles than OBP2.

may be crucial to the protein chemoreceptive function. In other words, the increased expression and binding affinity of the CSP1 to floral volatiles at low temperatures collectively enhance the ability of *A. cerana* to recognize volatiles of loquat flowers during the early winter season.

5. Conclusion

The present study identified a dual sensing mechanism whereby low temperatures upregulated the expression of CSP1 and enhanced its binding affinity to the volatiles of loquat flowers in early winter. The binding mechanism mainly depends on the type of specific volatile molecule rather than the type of olfactory soluble protein. F44 is a key amino acid in the binding process of CSP1 to three ligands. These research findings provide a theoretical foundation for understanding the molecular mechanism by which *A. cerana* perceives native flowering plants in early winter. Moreover, this study offers significant theoretical insights into the co-evolution of low-temperature adaptation between *A. cerana* and flowering plants in natural habitats.

CRediT authorship contribution statement

Jia-Qi Huang: Writing – original draft, Investigation. **Li Zhang:** Writing – original draft, Investigation. **Fan Wu:** Methodology, Investigation. **Jing Tan:** Investigation, Data curation. **Ping Wen:** Visualization, Methodology. **Wei Xu:** Writing-review & editing. **Hong-Liang Li:** Writing – review & editing, Supervision, Resources, Project administration, Funding acquisition.

Declaration of competing interest

The authors declared that they have no conflicts of interest to this work. We declare that we do not have any commercial or associative interest that represents a conflict of interest in connection with the work submitted.

Acknowledgments

This work was supported by the National Natural Science Foundation of China (No. 32170531), the National Key Research and Development Program of China (2023YFE0104800), and the Three Agricultural Nine-party Science and Technology Collaboration Projects of Zhejiang Province (2023SNJF053).

Appendix A. Supplementary data

Supplementary data to this article can be found online at https://doi.org/10.1016/j.bbadis.2024.167601.

Data availability

Data will be made available on request.

References

[1] S.E. Radloff, C. Hepburn, H.R. Hepburn, S. Fuchs, S. Hadisoesilo, K. Tan, M. S. Engel, Population structure and classification of *Apis cerana*, Apidologie 41 (6) (2010) 589–601.
[2] K.S. Ahmed, T. Muhammad, A. Saboor, M. Messaoud, N. Muhammad, N. Zeenat, S. Wiebke, D. Claudia, G. Dave, Declining abundance of pollinating insects drives falls in loquat (*Eriobotrya japonica*) fruit yields in the Pothwar region of Pakistan, Agr Ecosyst Environ 339 (2022) 108138.
[3] B.P. Oldroyd, S. Wongsiri, Asian Honey Bees: Biology, Conservation, and Human Interactions, Harvard University Press, 2006.
[4] A. Saboor, K. Ahlam, K.S. Ahmed, K.K. Ali, J.M. Jawad, H. Taimoor, S. Milan, A GH, Zubair A., Effects of native pollinator communities on the physiological and chemical parameters of loquat tree (*Eriobotrya japonica*) under open field condition, Saudi Journal of Biological Sciences 28 (6) (2021) 3235–3241.
[5] J. Dong, M.J. Huang, H. Zhang, S.Y. Yang, Evaluation of effect of pollination by different bees on improving quality and yield of loquat fruit (*Eriobotrya japonica*) in Qiandao Lake region (in Chinese), Apiculture of China 75 (01) (2024) 53–56.
[6] R.V.M. Lerner, Two groups of odorant binding proteins in insects suggest specific and general olfactory pathways, Neurosci Abstr 15 (1989) 1290–1296.
[7] K.N. Slessor, L.A. Kaminski, G.G.S. King, J.H. Borden, M.L. Winston, Semiochemical basis of the retinue response to queen honey bees, Nature 332 (6162) (1988) 354–356.
[8] P. Pelosi, I. Iovinella, A. Felicioli, F.R. Dani, Soluble proteins of chemical communication: an overview across arthropods, Front. Physiol. 5 (2014) 320.
[9] W.S. Leal, Odorant reception in insects: roles of receptors, binding proteins, and degrading enzymes, Annu. Rev. Entomol. 58 (1) (2013) 373–391.
[10] Li HL, Gao QK, Cheng JA. Analysis of spatio-temporal expression of two kinds of proteins related to chemical communication in *Apis cerana cerana* (Hymenoptera: Apidae) (in Chinese, In Press). Journal of Agricultural and Biotechnology (First-Class Journal in China), 2008.
[11] H.L. Li, X.M. Song, F. Wu, Y.L. Qiu, X.B. Fu, L.Y. Zhang, J. Tan, Chemical structure of semiochemicals and key binding sites together determine the olfactory functional modes of odorant-binding protein 2 in eastern honey bee, Apis cerana. Int J Biol Macromol 145 (2020) 876–884.
[12] L. Zhang, H.Q. Jiang, F. Wu, P. Wen, J. Qing, X.M. Song, H.L. Li, Eastern honeybee *Apis cerana* sense cold flowering plants by increasing the static binding affinity of odorant-binding protein to cold floral volatiles from loquats, Int. J. Biol. Macromol. 123227 (2023).
[13] H.L. Li, C.X. Ni, J. Tan, L.Y. Zhang, F.L. Hu, Chemosensory proteins of the eastern honeybee, *Apis cerana*: identification, tissue distribution and olfactory related functional characterization, Comp Biochem Phys B 194-195 (2016) 11–19.
[14] J. Tan, X.M. Song, X.B. Fu, F. Wu, F.L. Hu, H.L. Li, Combinatorial multispectral, thermodynamics, docking and site-directed mutagenesis reveal the cognitive characteristics of honey bee chemosensory protein to plant semiochemical, Spectrochimica Acta Part a-Molecular and Biomolecular Spectroscopy 201 (2018) 346–353.
[15] H.L. Li, J. Tan, X.M. Song, F. Wu, M.Z. Tang, Q.Y. Hua, H.Q. Zheng, F.L. Hu, Sublethal doses of neonicotinoid imidacloprid can interact with honey bee chemosensory protein 1 (CSP1) and inhibit its function, Biochem Bioph Res Co 486 (2017) 391–397.
[16] L. Ban, A. Scaloni, C. D'Ambrosio, L. Zhang, Y. Yan, P. Pelosi, Biochemical characterization and bacterial expression of an odorant-binding protein from Locusta migratoria, Cellular & Molecular Life Sciences 60 (2) (2003) 390–400.
[17] Z. Chi, J. Zhao, H. You, M. Wang, Study on the mechanism of interaction between phthalate acid esters and bovine hemoglobin, J. Agric. Food Chem. 64 (30) (2016) 6035–6041.

[18] L. Zhang, F. Jin, T. Zhang, L. Zhang, J. Xing, Structural influence of graft and block polycations on the adsorption of BSA, Int. J. Biol. Macromol. 85 (2016) 252–257.
[19] N.H. Guo, C.L. Wang, C. Shang, X. You, L.Y. Zhang, W.B. Liu, Integrated study of the mechanism of tyrosinase inhibition by baicalein using kinetic, multispectroscopic and computational simulation analyses, Int. J. Biol. Macromol. 118 (Pt A) (2018) 57–68.
[20] Y.-J. Hu, Y. Liu, L.-X. Zhang, R.-M. Zhao, S.-S. Qu, Studies of interaction between colchicine and bovine serum albumin by fluorescence quenching method, J. Mol. Struct. 750 (1) (2005) 174–178.
[21] A. Konstantin, B. Lorenza, K. Jürgen, S. Torsten, The SWISS-MODEL workspace: a web-based environment for protein structure homology modelling, Bioinformatics 22 (2) (2006) 195–201.
[22] W. Zhang, Z. Liu, M. Zhu, L. Ma, Y. Wang, H. Wang, X. Guo, B. Xu, Molecular cloning, expression and oxidative stress response of the vitellogenin gene (AccVg) from *Apis cerana cerana*, Apidologie 48 (5) (2017) 599–611.
[23] Y. Zhang, Y. Liu, X. Guo, Y. Li, H. Gao, X. Guo, B. Xu, sHsp22.6, an intronless small heat shock protein gene, is involved in stress defence and development in *Apis cerana cerana*, Insect Biochem. Mol. Biol. 53 (2014) 1–12.
[24] Z. Wang, F. Yang, A. Sun, S. Shan, Y. Zhang, S. Wang, Expression profiles and functional characterization of chemosensory protein 15 (HhalCSP15) in the brown marmorated stink bug *Halyomorpha halys*, Front. Physiol. 12 (2021) 721247.
[25] Z. Wang, F. Yang, A. Sun, J. Song, S. Shan, Y. Zhang, S. Wang, Expressional and functional comparisons of five clustered odorant binding proteins in the brown marmorated stink bug *Halyomorpha halys*, Int. J. Biol. Macromol. 206 (2022) 759–767.
[26] C. Zhang, B. Tang, T. Zhou, X. Yu, M. Hu, W. Dai, Involvement of chemosensory protein BodoCSP1 in perception of host plant volatiles in *Bradysia odoriphaga*, J. Agric. Food Chem. 69 (37) (2021) 10797–10806.
[27] J. Jiang, J. Xue, M. Yu, X. Jiang, Y. Cheng, H. Wang, Y. Liu, W. Dou, J. Fan, J. Chen, Molecular characterization of chemosensory protein (CSP) genes and the involvement of AgifCSP5 in the perception of host location in the aphid parasitoid *Aphidius gifuensis*, Int. J. Mol. Sci. 25 (12) (2024).
[28] G.W. Li, X.L. Chen, L.H. Chen, W.Q. Wang, J.X. Wu, Functional analysis of the chemosensory protein GmolCSP8 from the oriental fruit moth, *Grapholita molesta* (Busck) (Lepidoptera: Tortricidae), Front. Physiol. 10 (2019) 552.
[29] H.L. Li, L.Y. Zhang, C.X. Ni, H.W. Shang, S.L. Zhuang, J.K. Li, Molecular recognition of floral volatile with two olfactory related proteins in the Eeastern honeybee (*Apis cerana*), Int. J. Biol. Macromol. 56 (1) (2013) 114–121.